Uncertainties in Seismic Moment Tensors Inferred from Differences between Global Catalogs

Boris Rösler[1], Seth Stein[1,2], and Bruce D. Spencer[2,3]

Abstract

Catalogs of moment tensors form the foundation for a wide variety of seismological studies. However, assessing uncertainties in the moment tensors and the quantities derived from them is difficult. To gain insight, we compare 5000 moment tensors in the U.S. Geological Survey (USGS) and the Global Centroid Moment Tensor (Global CMT) Project catalogs for November 2015–December 2020 and use the differences to illustrate the uncertainties. The differences are typically an order of magnitude larger than the reported errors, suggesting that the errors substantially underestimate the uncertainty. The catalogs are generally consistent, with intriguing differences. Global CMT generally reports larger scalar moments than USGS, with the difference decreasing with magnitude. This difference is larger than and of the opposite sign from what is expected due to the different definitions of the scalar moment. Instead, the differences are intrinsic to the tensors, presumably in part due to different phases used in the inversions. The differences in double-couple components of source mechanisms and the fault angles derived from them decrease with magnitude. Non-double-couple (NDC) components decrease somewhat with magnitude. These components are moderately correlated between catalogs, with correlations stronger for larger earthquakes. Hence, small earthquakes often show large NDC components, but many have large uncertainties and are likely to be artifacts of the inversion. Conversely, larger earthquakes are less likely to have large NDC components, but these components are typically robust between catalogs. If so, these can indicate either true deviation from a double couple or source complexity. The differences between catalogs in scalar moment, source geometry, or NDC fraction of individual earthquakes are essentially uncorrelated, suggesting that the differences reflect the inversion rather than the source process. Despite the differences in moment tensors, the location and depth of the centroids are consistent between catalogs. Our results apply to earthquakes after 2012, before which many moment tensors were common to both catalogs.

Cite this article as Rösler, B., S. Stein, and B. D. Spencer (2021). Uncertainties in Seismic Moment Tensors Inferred from Differences between Global Catalogs, *Seismol. Res. Lett.* **92**, 3698–3711, doi: 10.1785/0220210066.

Introduction

The availability of large volumes of digital seismic data enabled the compilation of catalogs of seismic moment tensors, which have become a powerful tool for a wide variety of studies in seismology and tectonics. However, assessing the uncertainties in the moment tensors and the quantities derived from them, which is important for characterizing the uncertainties in studies that make use of them, is difficult.

The difficulty in assessing uncertainties reflects the complexity of the process of determining moment tensors by inverting the waveforms or spectra of seismic waves. The results depend on the type and frequency of the waves used in the inversion, the specifics of the inversion algorithm, Earth structure parameters used in the inversion, and the quantity and quality of the data used. Not surprisingly, differences arise between moment tensors and the quantities derived from them found by different studies. We use the differences between the results of different studies as a proxy for their uncertainty. This approach is useful when uncertainties are difficult to assess formally owing to the complexity of the analysis process (e.g., Neely *et al.*, 2020).

1. Department of Earth and Planetary Sciences, Northwestern University, Evanston, Illinois, U.S.A., https://orcid.org/0000-0001-8596-5650 (BR); https://orcid.org/0000-0003-0522-7418 (SS); 2. Institute for Policy Research, Northwestern University, Evanston, Illinois, U.S.A., https://orcid.org/0000-0001-6155-7249 (BDS); 3. Department of Statistics, Northwestern University, Evanston, Illinois, U.S.A.

*Corresponding author: boris@earth.northwestern.edu

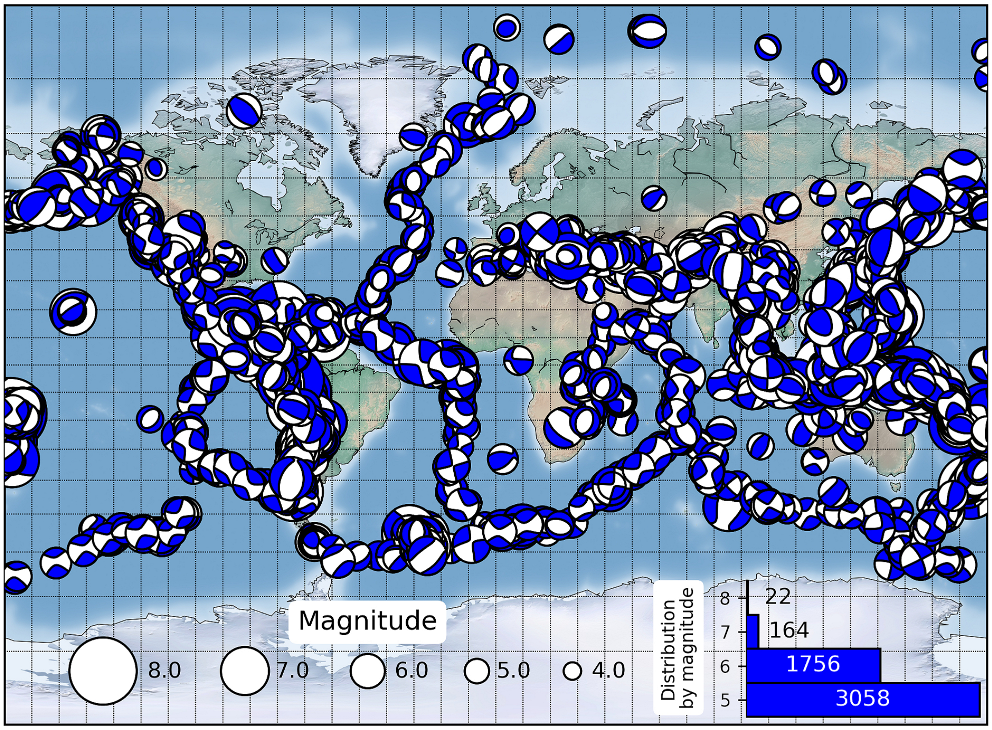

Figure 1. Location and focal mechanisms of 5000 earthquakes with moment tensors in both catalogs. The earthquakes have magnitudes between M_w 4.5 and 8.2 and occurred between November 2015 and December 2020. The color version of this figure is available only in the electronic edition.

correlation between the non-double-couple (NDC) components in the different catalogs. Kagan (2003) found that routinely determined NDC components are in most cases artifacts and that the fault angles of the double-couple (DC) component have uncertainties of less than 10°. Hayes *et al.* (2009) and Duputel, Rivera, Kanamori, *et al.* (2012) found good agreement between the moment magnitudes and the moment tensors in the USGS and Global CMT catalogs.

This article builds on earlier studies by comparing the moment tensors and various quantities derived from them for 5000 earthquakes from November 2015 to December 2020 that appear in both the Global CMT Project and the USGS catalogs (Fig. 1). We use this recent period because prior to 2012 the USGS catalog included many solutions from the Global CMT catalog, whereas the moment tensors in our study were independently determined. We identify corresponding events in both catalogs by their source time (±60 s), location (difference of less than 1°), and magnitude ($M_w \pm 0.5$). The difference in magnitude lets us examine differences in scalar moment between catalogs. The earthquakes have a range of tectonic settings and magnitudes above M_w 4.5.

An analogous approach has been used by studies that addressed uncertainties in origin time, location, or magnitude by comparing results between earthquake catalogs (Smith and Ekström, 1997; Harte and Vere-Jones, 1999; Röhm *et al.*, 1999; Storchak *et al.*, 2000). With the advent of moment tensor catalogs, results derived from moment tensors were compared with ones from other methods. Dziewonski and Woodhouse (1983) compared locations in the then-new Global Centroid Moment tensor (Global CMT) catalog with those derived from travel times in the U.S. Geological Survey's (USGS) Preliminary Determination of Epicenters (PDEs) catalog. Engdahl *et al.* (1998) considered global and regional hypocenter differences in the International Seismological Centre and PDE catalogs and relocated nearly 100,000 hypocenters. They also analyzed differences in location and depth between the relocated solutions and moment tensors in the Global CMT catalog.

Once multiple moment tensor solutions for the same earthquakes became available, the differences between them have been used to explore their uncertainties. Helffrich (1997) used radiation-pattern correlation coefficients to compare moment tensors in the USGS, Global CMT, and Earthquake Research Institute catalogs and found that slip vectors of typical shallow earthquakes had an uncertainty of 14°. Frohlich and Davis (1999) studied focal mechanisms in different catalogs and found similar uncertainty. Moreover, they found very low

Moment Tensors

Seismic waves generated by an earthquake are linearly related to the earthquake's moment tensor, so can be inverted to infer the moment tensor (Gilbert, 1971; Gilbert and Dziewonski, 1975; McCowan, 1976; Mendiguren, 1977). The moment tensor, which describes the seismic source in terms of nine force couples that generate the seismic waves, is more general than assuming a DC source representing slip on a fault plane described by its strike, dip, and slip angles.

Moment tensors can be expressed as the product of the scalar moment M_0 and a normalized tensor

$$\underline{\underline{M}} = M_0 \begin{pmatrix} M_{rr} & M_{r\theta} & M_{r\varphi} \\ M_{\theta r} & M_{\theta\theta} & M_{\theta\varphi} \\ M_{\varphi r} & M_{\varphi\theta} & M_{\varphi\varphi} \end{pmatrix}. \quad (1)$$

The scalar moment, which measures the earthquake's size, corresponds to the traditional product of area, slip distance, and rigidity for slip on a fault, but it can include contributions from NDC components of the source. The normalized tensor contains information on the geometry of the source, again including both DC and NDC components.

Moment tensors can be decomposed into components representing different physical processes. Diagonalization yields a moment tensor with eigenvalues λ_1, λ_2, and λ_3 on its diagonal, in which $\lambda_1 > \lambda_3 > \lambda_2$. Subtracting a diagonal matrix with components equal to the isotropic moment $M^{\text{iso}} = (\lambda_1 + \lambda_2 + \lambda_3)/3$, representing the source's volumetric change, yields the deviatoric moment tensor with eigenvalues λ_1', λ_2', and λ_3' that is typically reported in catalogs. This has no net volume change because its trace, the sum of its eigenvalues, $\lambda_1' + \lambda_2' + \lambda_3' = 0$. The deviatoric tensor is typically decomposed into a DC component describing slip on a fault and an NDC component that represents either other source processes or artifacts of the inversion process. However, this decomposition is not unique.

One decomposition is in terms of major and minor DCs (e.g., Kanamori and Given, 1981), each with two equal and opposite eigenvalues:

$$\begin{pmatrix} \lambda_1' & 0 & 0 \\ 0 & \lambda_2' & 0 \\ 0 & 0 & \lambda_3' \end{pmatrix} = \begin{pmatrix} \lambda_1' & 0 & 0 \\ 0 & -\lambda_1' & 0 \\ 0 & 0 & 0 \end{pmatrix} + \begin{pmatrix} 0 & 0 & 0 \\ 0 & -\lambda_3' & 0 \\ 0 & 0 & \lambda_3' \end{pmatrix}. \quad (2)$$

Typically, $|\lambda_1'|$ is much larger than $|\lambda_3'|$, so the major DC is treated as the earthquake's DC source mechanism and the minor DC is considered the NDC component.

Another common decomposition (Knopoff and Randall, 1970) is

$$\begin{pmatrix} \lambda_1' & 0 & 0 \\ 0 & \lambda_2' & 0 \\ 0 & 0 & \lambda_3' \end{pmatrix} = (\lambda_1' + 2\lambda_3') \begin{pmatrix} 1 & 0 & 0 \\ 0 & -1 & 0 \\ 0 & 0 & 0 \end{pmatrix} + \lambda_3' \begin{pmatrix} -2 & 0 & 0 \\ 0 & 1 & 0 \\ 0 & 0 & 1 \end{pmatrix}. \quad (3)$$

In this decomposition, the NDC component is a compensated linear vector dipole (CLVD). A CLVD is a set of three force dipoles that are compensated, with one dipole twice the magnitude of the others and no change in volume. The polarity of λ_3' indicates whether there are two axes of compression and one of dilatation or the opposite.

Moment tensors found by inversions typically have three nonzero eigenvalues. Most are dominated by their DC components and have a smaller NDC component, so $\lambda_1' \approx -\lambda_2'$ and $|\lambda_1'| \gg \lambda_3'$. For a pure DC, $\lambda_3' = 0$ and $\lambda_1' = -\lambda_2'$. The ratio of the smallest and largest eigenvalues $\epsilon = \lambda_3' / \max(|\lambda_1'|, |\lambda_2'|)$ is often used to quantify the deviation of the source mechanism from a DC source (Dziewonski *et al.*, 1981).

The different formulations for the DC and NDC components reflect the fact that the moment tensor represents a force system, so different decompositions can reflect the same net force system and thus generate the same seismic waves. Hence, the seismic waves alone cannot distinguish between alternative decompositions.

Differences in Moment Tensors

The differences between moment tensors can be characterized by differences between their components. The errors reported for the components can be useful when assessing relative uncertainty between components. However, these reported errors reflect only the misfit of the source model to the data but do not include the uncertainty due to the inversion procedure (Dziewonski *et al.*, 1981; Duputel, Rivera, Fukahata, *et al.*, 2012). Seismograms are a linear combination of Green's functions weighted by the components of the moment tensor. Hence, moment tensor components are determined via an inverse problem by finding the best fit to the data given the assumed Green's functions. Thus, the results depend on specific aspects of the inversion process including the portions of the wavefield inverted, the Earth model for elastic and anelastic structure assumed (Šílený, 2004; Cesca *et al.*, 2006; Rößler *et al.*, 2007), noise in the data (Šílený *et al.*, 1996; Jechumtálová and Šílený, 2001), and the number of seismic stations and their azimuthal coverage (Cesca *et al.*, 2006; Ford *et al.*, 2010; Vera Rodriguez *et al.*, 2011; Domingues *et al.*, 2013).

USGS does not routinely report errors, whereas Global CMT reports errors derived from misfits to the data (Dziewonski *et al.*, 1981; G. Ekström, personal comm., 2021). To compare these errors with the differences in moment tensors between catalogs, we use the root mean square ratio of the differences in components between catalogs to the errors reported by Global CMT,

$$\rho \equiv \sqrt{\frac{1}{6} \sum_{i=1}^{3} \sum_{j=i}^{3} \left(\frac{M_{ij}^{\text{USGS}} - M_{ij}^{\text{Global CMT}}}{\Delta M_{ij}^{\text{Global CMT}}} \right)^2}. \quad (4)$$

For the 5000 earthquakes in our study, the difference between catalogs is much larger than the reported errors (Fig. 2a), implying that the reported error underestimates the uncertainties in the moment tensor by more than an order of magnitude. The reported errors underestimate the uncertainties in source mechanism for large earthquakes more than for small earthquakes (Fig. 2b). Hence, the reported errors inferred from the misfit probably substantially underestimate the full uncertainty in determining moment tensors and hence aspects of the source.

We next explore the resulting differences between quantities derived from the moment tensors, which have physical significance and thus are often used.

Differences in Scalar Moments

Differences in the moment tensor and derived quantities for a given earthquake between catalogs can arise either from different definitions of quantities or from the inversion process.

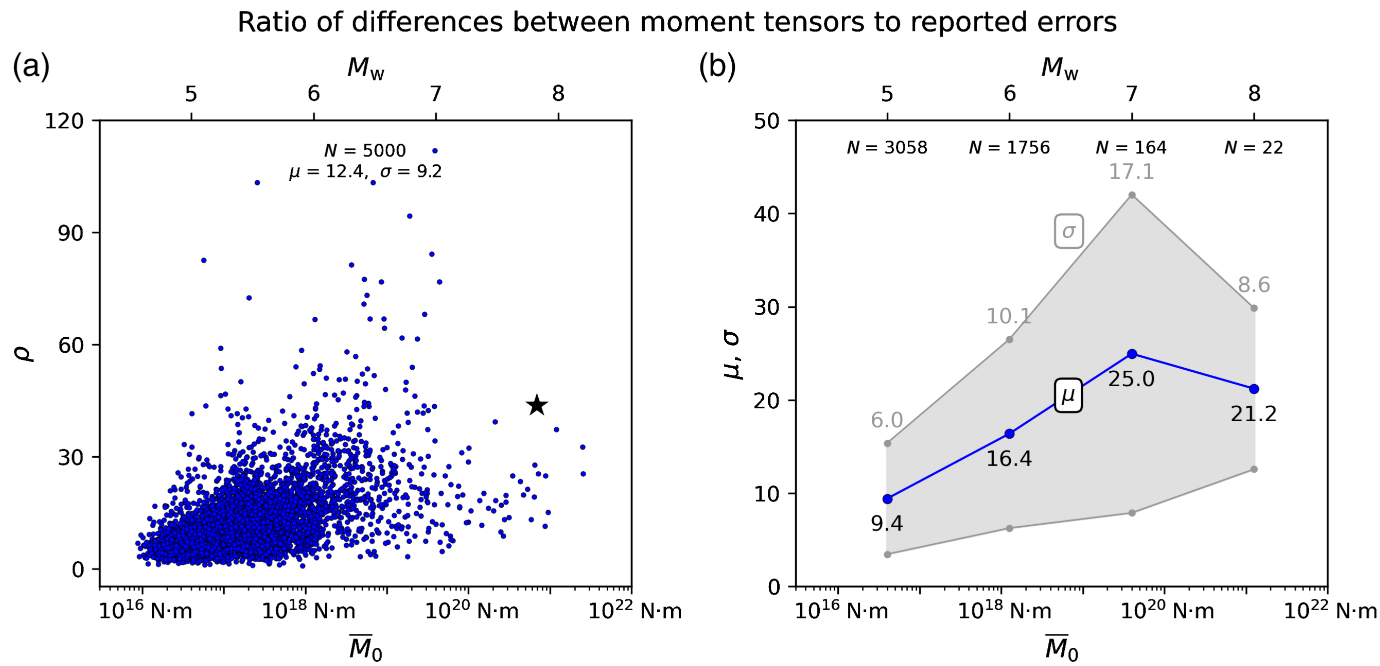

Figure 2. (a) Root mean square ratio of differences between moment tensors and errors reported by the Global Centroid Moment Tensor (Global CMT) Project, showing that the differences are approximately an order of magnitude greater. The star represents the 2016 Kaikōura earthquake. (b) The ratio, given for one magnitude unit bins, for example, 4.5–5.5, increases with magnitude, indicating that the reported errors underestimate the uncertainties for large earthquakes more than for small earthquakes. The color version of this figure is available only in the electronic edition.

Scalar moments, as the best indicator of earthquake size, are among the most widely used source parameters. The scalar moment can be calculated from a moment tensor in different ways (Vavryčuk, 2015). The USGS defines the scalar moment as the Euclidian norm of the moment tensor (Silver and Jordan, 1982),

$$M_0^{\mathrm{USGS}} = \sqrt{\frac{1}{2}\sum_{i=1}^{3}\sum_{j=i}^{3} M_{ij}^2} = \sqrt{\lambda_1'^2 + \lambda_2'^2 + \lambda_3'^2}, \tag{5}$$

which includes the contribution of the NDC component. In contrast, Global CMT defines the scalar moment as the average of the two eigenvalues with largest absolute value, which yields the scalar moment of the best DC,

$$M_0^{\mathrm{Global\ CMT}} = \frac{1}{2}(|\lambda_1'| + |\lambda_2'|), \tag{6}$$

and does not include the NDC component. Hence, as shown in Figure 3, small differences in the scalar moment between catalogs are expected when a source deviates from a DC source ($\lambda_3' \neq 0$). The normalized scalar moment difference due to the definitions increases with the deviation of the source from a DC and amounts to about 0.2% for a deviation of 30%.

We thus first consider differences in the scalar moment reported in the two catalogs for the 5000 events (Fig. 1). The distribution of normalized scalar moment differences

$$\Delta M_0/\overline{M}_0 \equiv \frac{M_0^{\mathrm{USGS}} - M_0^{\mathrm{Global\ CMT}}}{\frac{1}{2}(M_0^{\mathrm{USGS}} + M_0^{\mathrm{Global\ CMT}})}, \tag{7}$$

has a negative mean (Fig. 4a), indicating that the scalar moment reported by Global CMT is generally larger than that in the USGS catalog. An omnibus test based on skew and kurtosis (d'Agostino, 1971) yields a vanishing two-sided chi-square probability that the distribution is Gaussian.

The differences generally decrease with the scalar moment (or moment magnitude) of an earthquake (Fig. 4b). The scalar moment reported by Global CMT is, on average, larger for small earthquakes. It appears that the scalar moments of small ($M_w < 6.5$) earthquakes from a global catalog should be viewed as known to about 10%. There is essentially no overall difference in moment between the catalogs for earthquakes of magnitude $M_w > 6.5$. The standard deviation of the differences also decreases with magnitude, presumably reflecting more consistent determination of source mechanisms for larger earthquakes, which is discussed later.

Are these differences due to the different definitions of the scalar moment? We compute the differences in scalar moment using the different definitions ($\Delta M_0^D/\overline{M}_0$) for both the moment tensors reported by the USGS and those reported by Global CMT (Fig. 5b). Both catalogs yield positive mean values, indicating that the USGS definition yields larger moments, as expected (Fig. 3). However, these differences in moment stemming from the definition are smaller than and have the opposite sign of the overall difference between the scalar moments (Fig. 4).

Thus, the differences between the scalar moments result from the tensors in the two catalogs, with Global CMT tensors

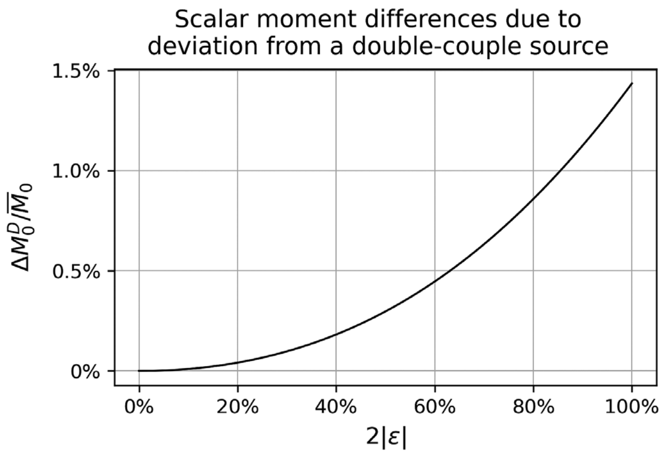

Figure 3. Effect of different definitions of the scalar moment. The U.S. Geological Survey (USGS) calculates the scalar moment as the norm of the moment tensor, whereas the Global CMT scalar moment is the best double-couple moment, neglecting the non-double-couple (NDC) component. Thus, the difference between definitions increases with the deviation from a double-couple source. The curve is identical for $\lambda_3' < 0$ and $\lambda_3' > 0$. However, $|\epsilon|$ depends on the sign of the smallest eigenvalue.

having, on average, larger scalar moments. Figure 5d shows the scalar moment differences between the tensors in the two catalogs ($\Delta M_0^C/\overline{M}_0$), computed using either the USGS or Global CMT definitions for the scalar moment. Both have negative means, confirming that the Global CMT tensors generally have larger scalar moments, regardless of the definition used to calculate the scalar moment.

For large earthquakes, the mean and standard deviation of the difference decreases (Fig. 5f), showing better agreement between moment tensors for larger earthquakes. The slight increase for the largest earthquakes presumably reflects the small number of earthquakes in the bin. This behavior is similar to the combined effect of differences resulting from the definition and those from the tensors themselves (Fig. 4b).

Differences in DC Components

For a DC source, the moment tensor's eigenvectors correspond to the principal stress axes. The T (least compressive), P (most compressive), and N (null) axes have eigenvalues λ_1', $\lambda_2' = -\lambda_1'$, and $\lambda_3' = 0$, respectively. We characterize the similarity between the DC components of the source mechanisms in the two catalogs using the angle Φ needed to rotate one set of axes into the other (Kagan, 1991). The mean rotation angle and its standard deviation decrease with magnitude (Fig. 6), showing that the inversions can yield relatively large differences for small earthquakes and are more consistent for larger earthquakes. Rotation angles of 10° are common for earthquakes of all magnitudes. The dataset includes the 2016 M_w 7.8 Kaikōura earthquake that ruptured different faults on the South Island of New Zealand. Interestingly, despite its complicated source process, the Kaikōura earthquake's rotation angle (10°) is not unusually large, indicating that its DC component is consistent between catalogs.

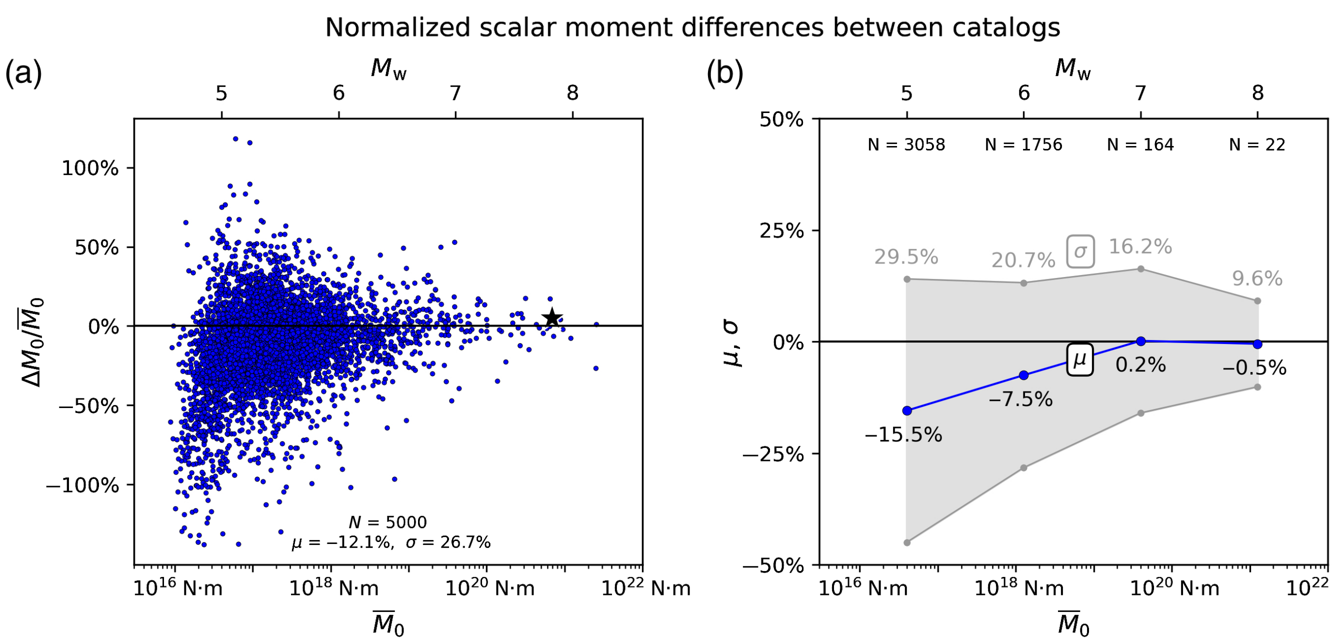

Figure 4. Differences in normalized scalar moment between catalogs for the same earthquakes. (a) The differences (USGS–Global CMT) have a negative mean, showing that the scalar moment in the Global CMT catalog is generally larger than that in the USGS catalog. The star marks the 2016 Kaikōura earthquake. (b) The differences, given for one magnitude unit bins, for example, 4.5–5.5, decrease with increasing mean moment or magnitude. The color version of this figure is available only in the electronic edition.

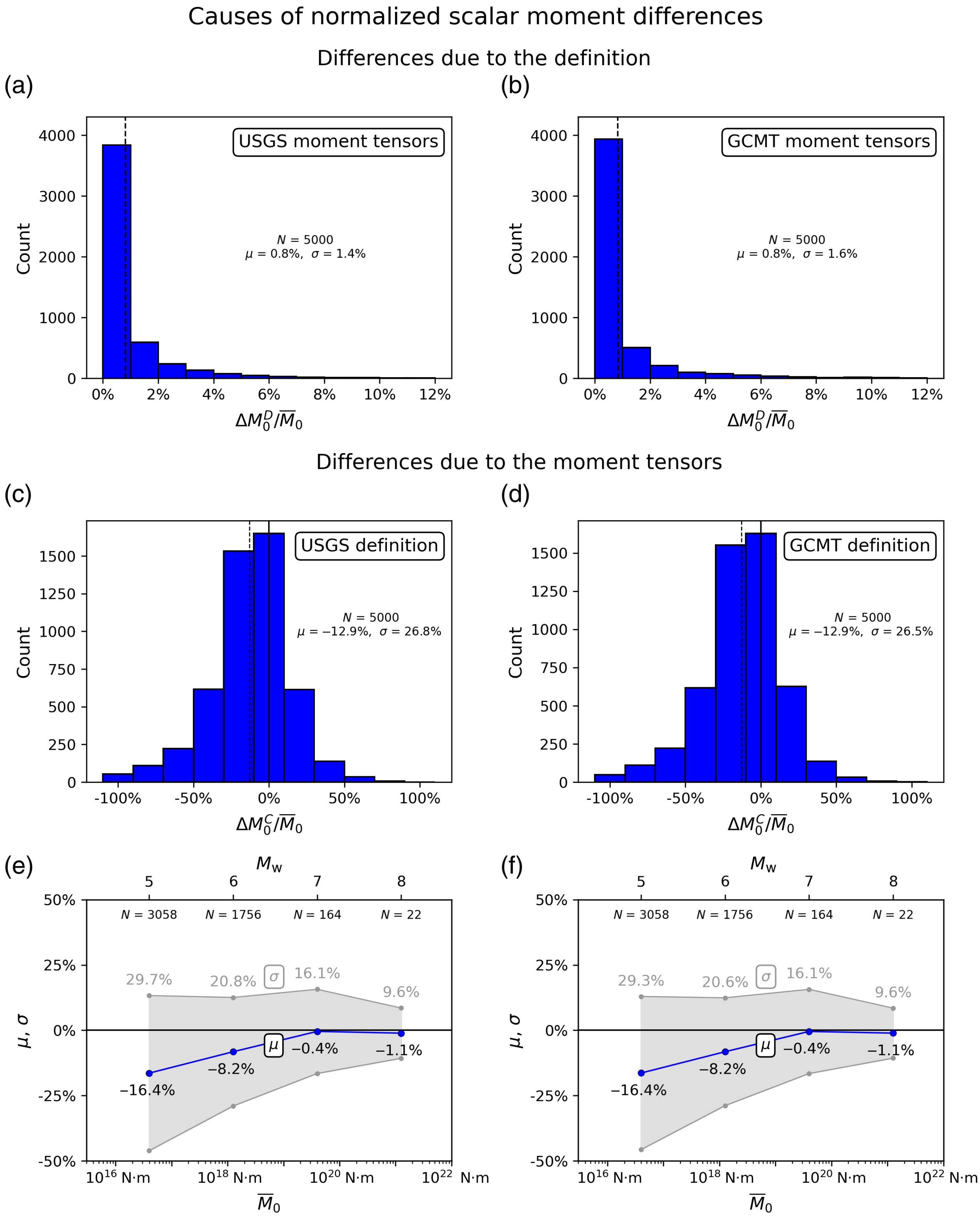

Figure 5. (a,b) Differences in scalar moment resulting from the definition of the scalar moment (ΔM_0^D), calculated for (a) USGS and (b) Global CMT moment tensors. Both distributions have positive means, confirming that the USGS definition yields larger values. (c,d) Differences (USGS–Global CMT) in scalar moment between tensors (ΔM_0^C). For both (c) USGS and (d) Global CMT definitions, Global CMT tensors have generally larger scalar moments. (e,f) Variation in the differences between catalogs (c, d) for different magnitude bins. The mean and standard deviations decrease with mean moment or magnitude. Values given are for one magnitude unit bins (e.g., 4.5–5.5). The color version of this figure is available only in the electronic edition.

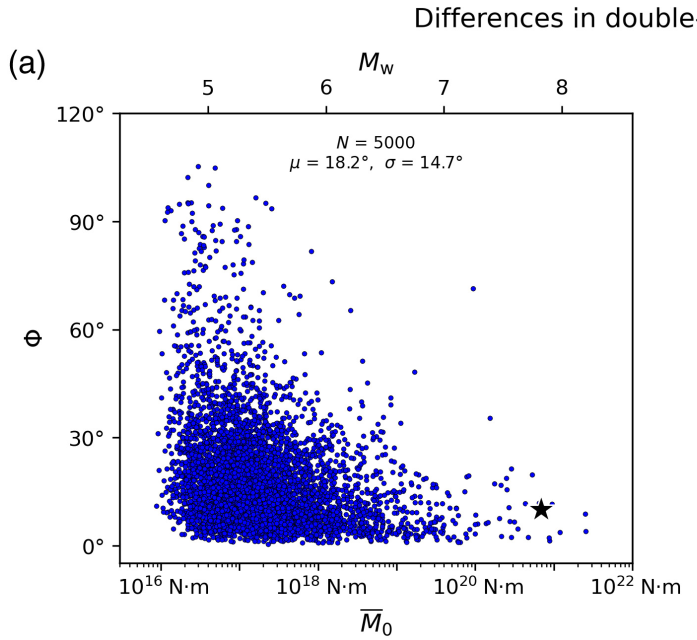

Figure 6. (a) Rotation angles between principal axes of the double-couple component of moment tensors in the two catalogs for the same earthquakes. Because of the symmetry of double-couple sources, the largest possible angle is 120°. (b) The mean rotation angle decreases with magnitude. Values given are for one magnitude unit bins (e.g., 4.5–5.5). The color version of this figure is available only in the electronic edition.

Differences in NDC Components

There has been considerable interest in whether the deviations from a DC source (non-double-couple components) are artifacts of the inversion or real source processes. Moreover, if they are real, what do they mean?

Real NDC components can result from various processes (Sipkin, 1986; Julian *et al.*, 1998; Miller *et al.*, 1998). In volcanic areas, a CLVD can describe an inflating magma dike, which can be modeled as a crack opening under tension (Nettles and Ekström, 1998). Alternatively, an NDC component can be due to the combined effects of near-simultaneous earthquakes on nearby faults of different geometries (e.g., Kawakatsu, 1991). These alternatives have been debated for earthquakes with NDC components in the Long Valley caldera region of California (Julian and Sipkin, 1985; Wallace, 1985; Sipkin, 1986). In non-volcanic areas, fault complexity seems the likely cause.

For this purpose, assessing the uncertainty in the NDC components is important. Figure 7 shows the deviation from a DC source, reported as $2|\epsilon|$ in the USGS catalog, for earthquakes in both catalogs. In both catalogs, the mean deviation from a DC source is 15%–25%, decreasing slightly with magnitude, as noted by Giardini (1984).

The mean difference in NDC components between the catalogs is small and varies little with magnitude (Fig. 8b), suggesting that there is no consistent bias between the catalogs in determining NDC components. However, because the eigenvalue with the smallest absolute value can be either negative or positive, the standard deviation of the difference between catalogs is fairly large and decreases with magnitude. The NDC components are moderately correlated between catalogs, indicating that the polarity of the NDC components is reliably determined by the inversion, although their size may vary between catalogs (Fig. 8d). The correlation increases drastically with magnitude, indicating that NDC components are more reliably determined for large earthquakes.

The decrease in NDC components with magnitude (Fig. 7) could reflect either smaller earthquakes being less dominated by slip on planar faults than large earthquakes or simply that the inversion results are less stable for small earthquakes. Larger earthquakes are expected to have complicated source geometries (e.g., Kawakatsu, 1991; Hayes *et al.*, 2010; Cirella *et al.*, 2012; Hamling *et al.*, 2017) that give rise to NDC components. The complex source process of the Kaikōura earthquake resulted in some of the largest NDC components in our dataset: 43% in the USGS catalog and 32% in the Global CMT catalog. Therefore, the decrease in difference between NDC components and their increase in correlation between catalogs (Fig. 8) suggest that inversion results for smaller earthquakes are less reliable and thus more likely to generate spurious NDC components.

Correlation of Differences in Source Parameters

The differences between catalogs in the reported scalar moments (Fig. 4), source geometry (rotation angle Φ) (Fig. 6), and NDC component (deviations from a DC source) (Fig. 8) all decrease with moment or magnitude. Hence, these quantities seem better resolved for large earthquakes, as

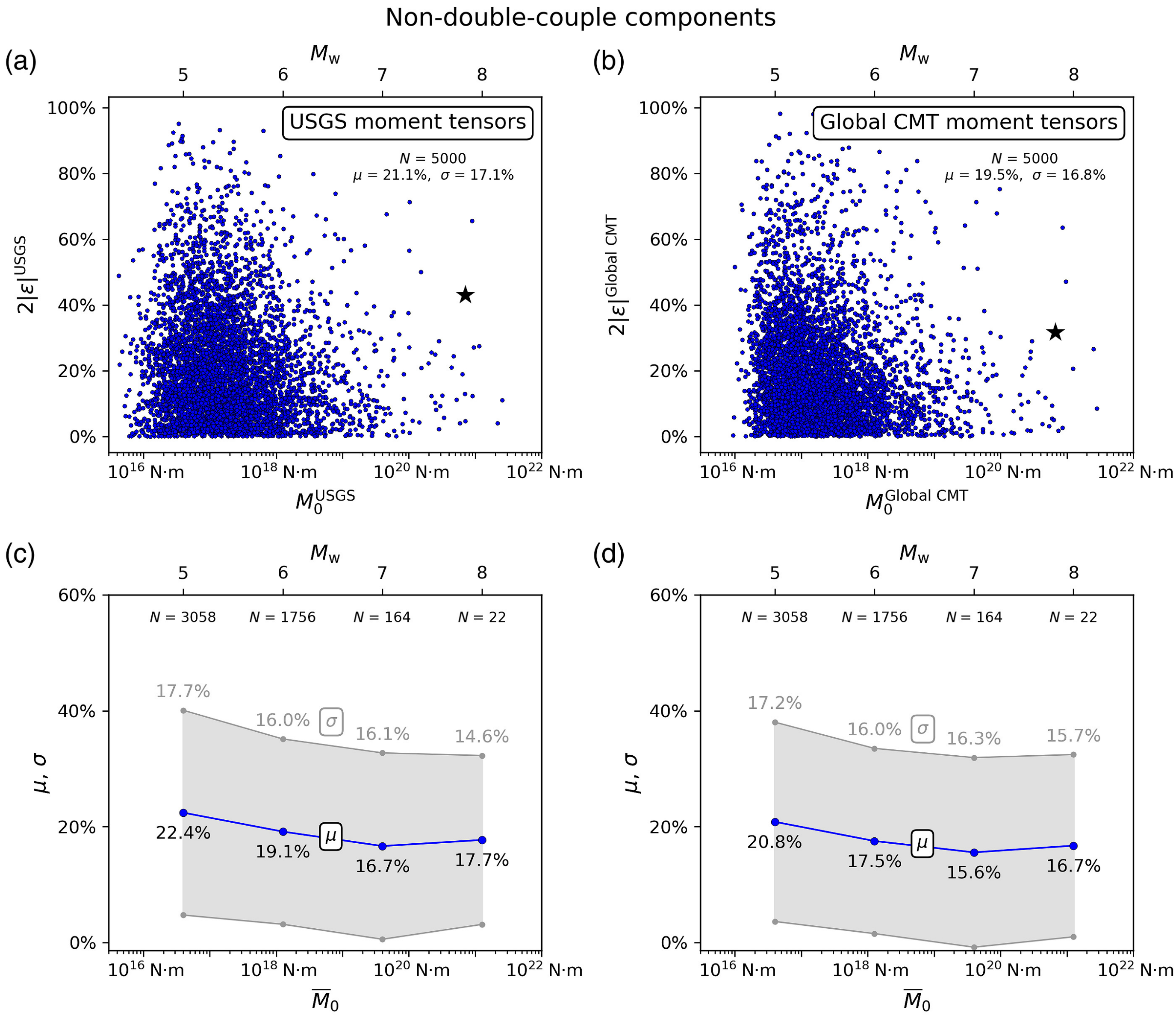

Figure 7. (a,b) Fractions of NDC components versus moment or magnitude for both catalogs. The star marks the 2016 Kaikōura earthquake. (c,d) Means and standard deviations of fractions of NDC components in different magnitude bins for USGS (c) and Global CMT (d) moment tensors. Values given are for one magnitude unit bins (e.g., 4.5–5.5). The color version of this figure is available only in the electronic edition.

expected. However, the differences between these three quantities in the two catalogs are uncorrelated (Fig. 9). Thus, the fact that one of these quantities is very similar between the two catalogs is unrelated to whether the other two are, implying that differences are artifacts of the inversions. For example, events for which one catalog contains a large NDC source are no more or less likely to have a scalar moment discrepancy.

Differences in Depth and Location

The location and depth of the centroids are obtained during a moment tensor inversion by minimizing the variance between observed and calculated waveforms or complex spectra. Despite the differences in moment tensors, the reported location and depth of the centroids are consistent between catalogs (Fig. 10). The overall differences in both location and depth are small. The difference in location is essentially constant, whereas the difference in depth decreases slightly with magnitude. For the Kaikōura earthquake, the differences in location (0.26°) and in depth (−3.3 km) are slightly larger than for earthquakes of similar size, reflecting the difficulties of assigning a single depth and location to earthquakes with complex rupture processes. Considering the different tectonic environments, which provide an unfavorable station coverage in azimuth and distance for some earthquakes, the coincidence in location and depth between catalogs is gratifying. However, a difference in location

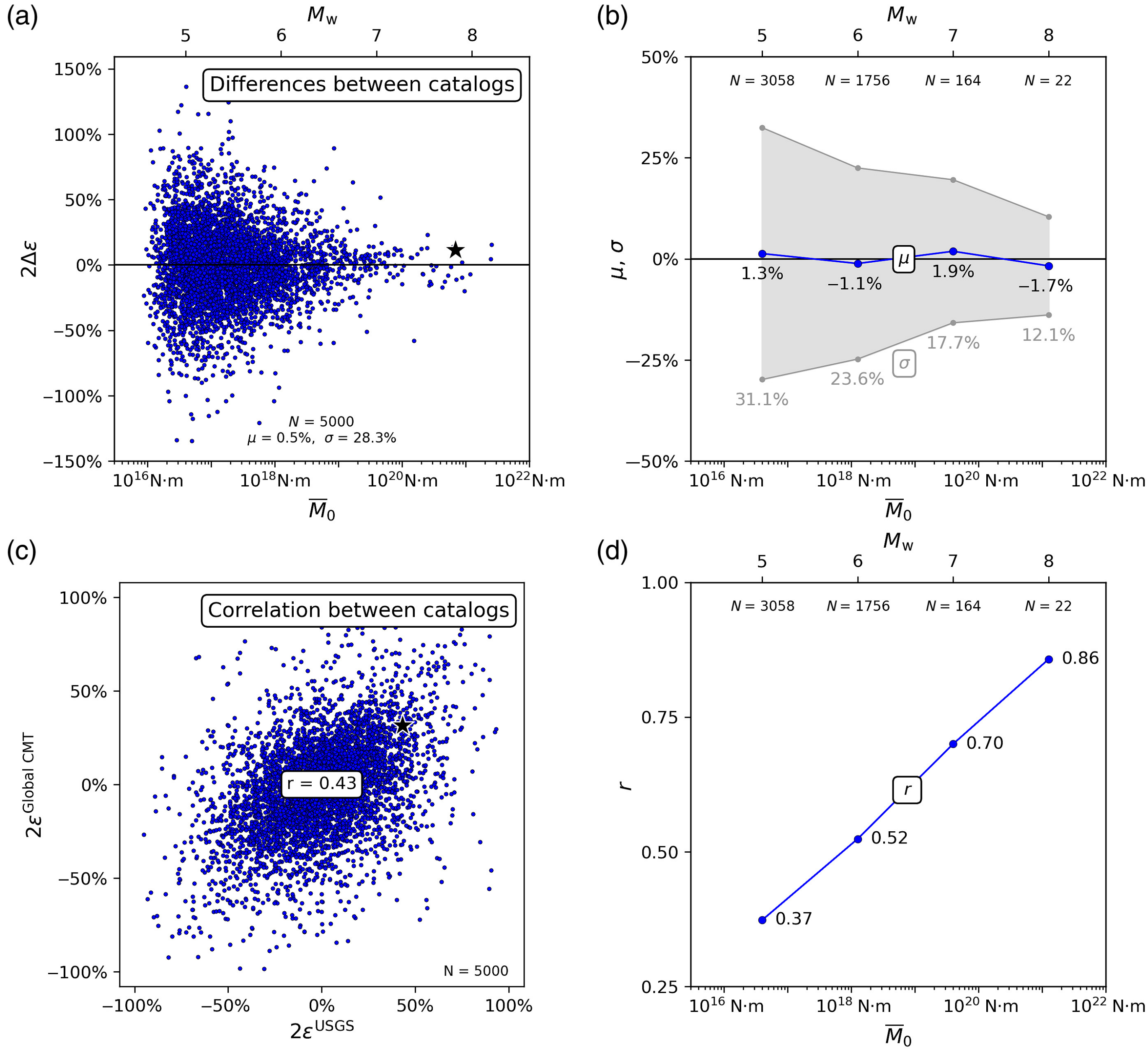

Figure 8. (a,b) Differences between NDC components between the USGS and Global CMT catalogs. Both have a small mean. The scatter of the differences between signed deviations is larger for small earthquakes than for large ones. Values given are for one magnitude unit bins (e.g., 4.5–5.5). (c,d) Correlation of NDC components between catalogs for all earthquakes and earthquakes in different magnitude bins. The star marks the 2016 Kaikōura earthquake. The color version of this figure is available only in the electronic edition.

of 20 km may be important for regional earthquake studies, typically involving events with $M_w < 6.5$.

Moment tensor inversions are generally based on long-period waves (e.g., Mendiguren, 1977; Kanamori and Given, 1981; Dziewonski and Woodhouse, 1983) because the amplitudes of body waves saturate for smaller earthquakes and due to a better signal-to-noise ratio, but constraints on the location and depth can be obtained from the first-arriving *P* wave (P. Earle, personal comm., 2021), increasing the stability of the inversion. When data are too poor to compute a reliable depth for an earthquake, the reported depth may be fixed. The USGS catalog contains 864 earthquakes at a depth of 11.5 km, and 1004 earthquakes have a depth of 12 km in the Global CMT catalog, which we assume to have been fixed. However, both the mean and standard deviation of the differences in depth change by less than 1 km if we discard earthquakes with a fixed depth in either catalog, showing that either depth is a reasonable choice for earthquakes with depths that cannot be determined during the inversion.

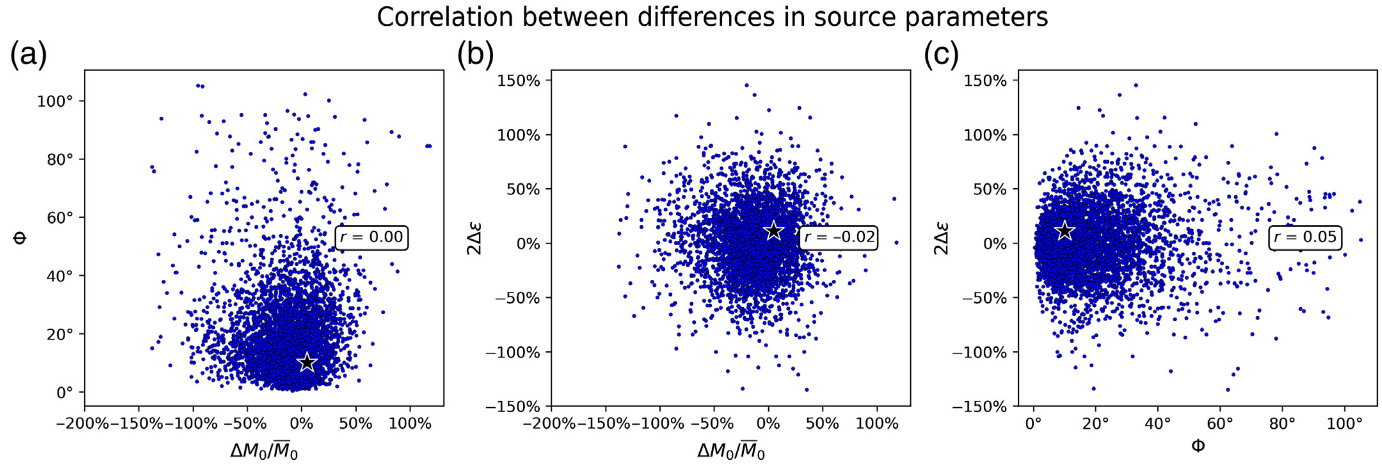

Figure 9. (a–c) Differences in scalar moment, source geometry (rotation angle Φ), and NDC component are uncorrelated between catalogs. The color version of this figure is available only in the electronic edition.

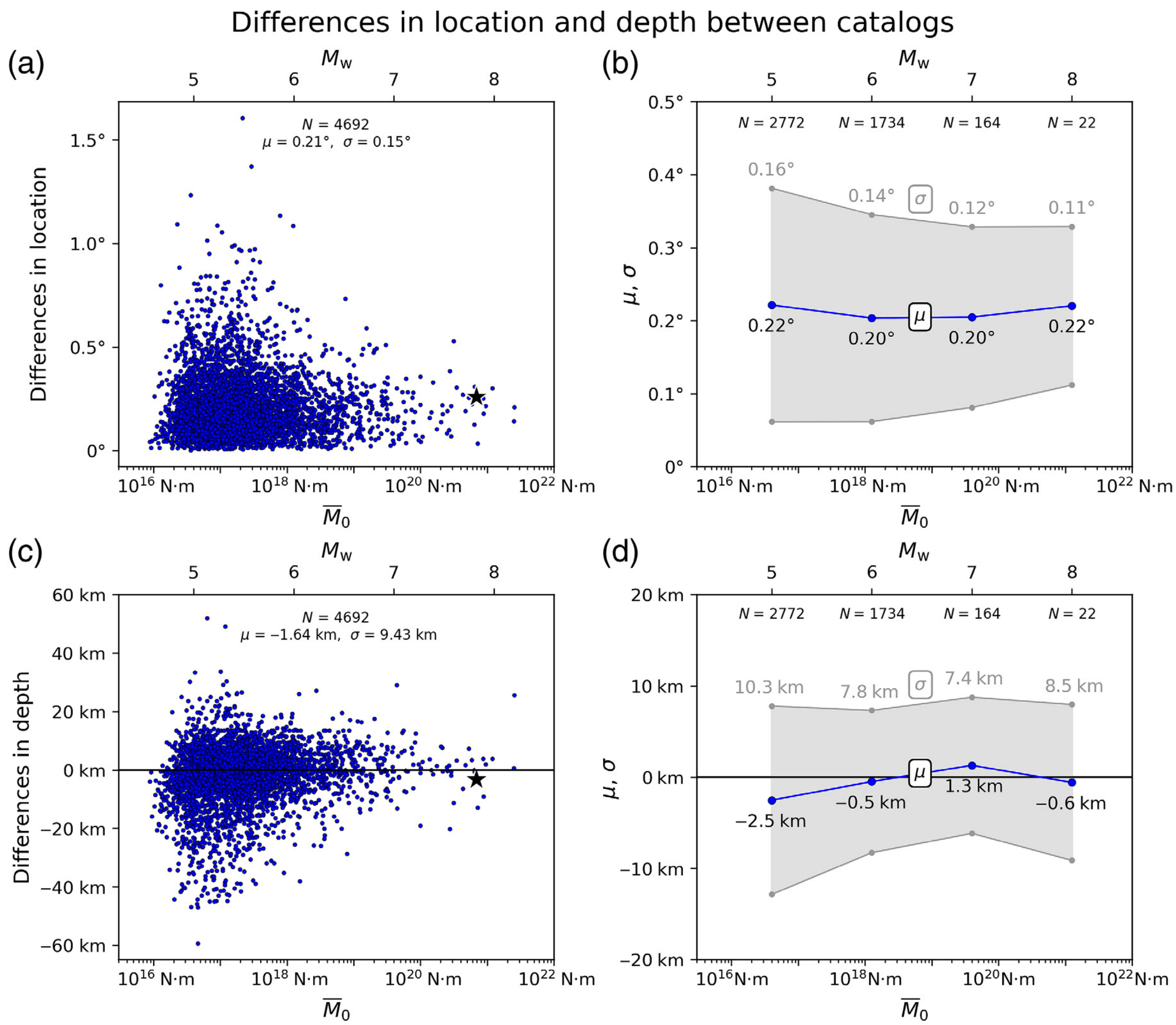

Figure 10. Differences in location and depth between catalogs. (a,b) The mean differences in location are small and independent of magnitude. (c,d) The mean differences in depth are small and decrease slightly with magnitude. The color version of this figure is available only in the electronic edition.

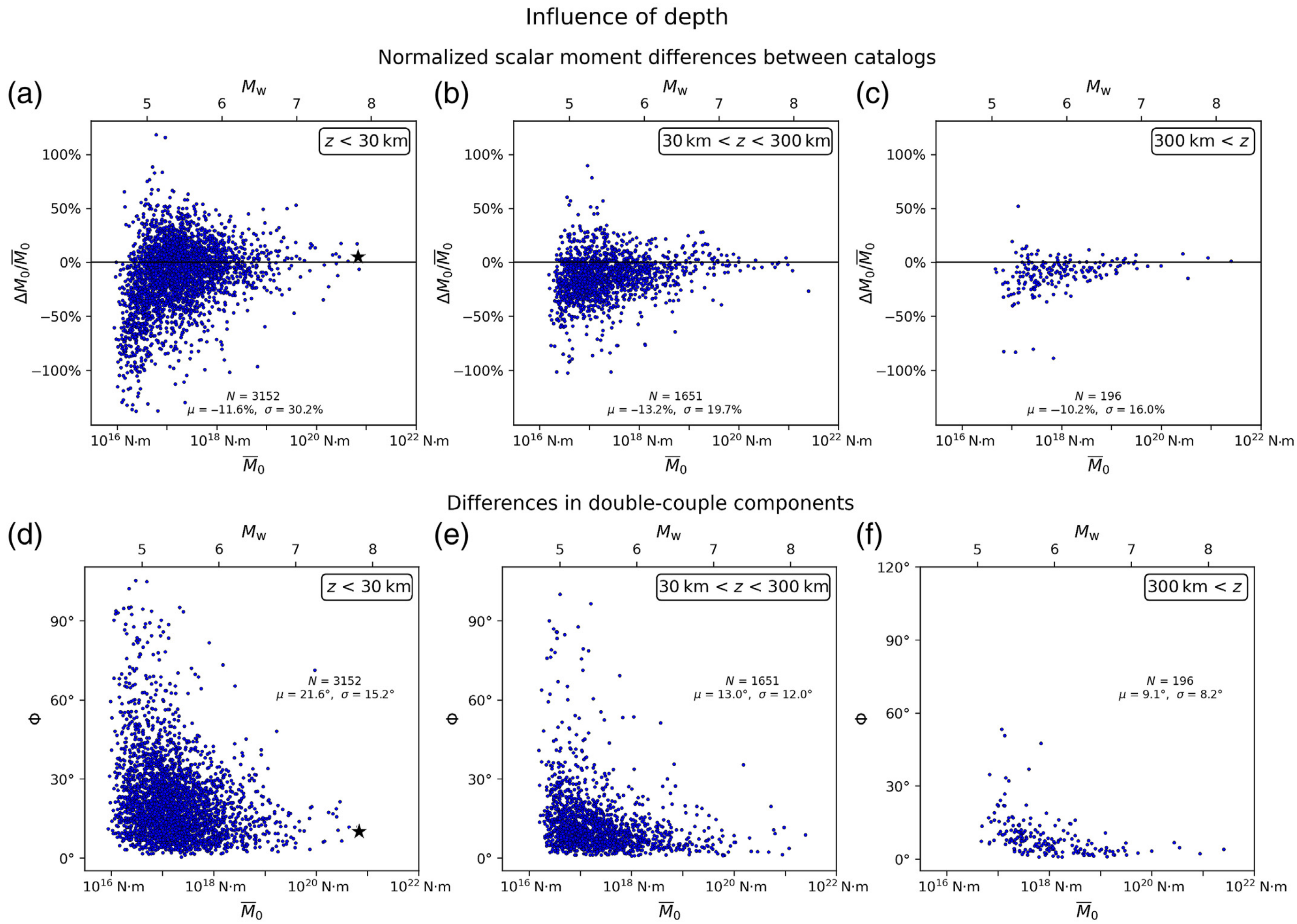

Figure 11. (a–c) Normalized scalar moment differences and (d–f) differences in double-couple components for shallow ($z < 30$ km), intermediate (30 km $< z <$ 300 km), and deep earthquakes (300 km $< z$). The standard deviation of both the normalized scalar moment differences and the differences between principal axes of the double-couple component (rotation angles) decrease with centroid depth. The color version of this figure is available only in the electronic edition.

Moment tensor solutions of shallow earthquakes are highly dependent on the frequency content of the waves used in the inversion (e.g., Hejrani and Tkalčić, 2020). Therefore, different inversions might yield larger differences for shallow earthquakes. We classify the earthquakes in our dataset as shallow if their centroid depth is less than 30 km and deep if their centroid depth is more than 300 km. Figure 11 shows that the standard deviation of the scalar moment differences decreases with depth (Fig. 11a–c), as does the standard deviation of the rotation angles (Fig. 11d–f). The decrease in standard deviation of the differences in deviation from a DC source (Fig. 12c) and the increased correlation between the NDC components (Fig. 12f) suggest better determination of source mechanisms for deep earthquakes.

Discussion and Conclusions

Comparison of moment tensors between catalogs gives insights into the uncertainties in the moment tensors and the quantities derived from them. The differences between catalogs are typically an order of magnitude larger than the reported errors. Hence, the reported errors, which reflect only the misfit of the source model to the data, substantially underestimate the uncertainty in estimates of aspects of the source due to the inversion procedure.

Moment tensors and the quantities derived from them are generally consistent between catalogs, with some intriguing differences. Some differences would be expected due to different data used in the inversions, different inversion procedures, and different Earth models. Global CMT uses body waves, surface waves, and mantle waves (very long period surface waves, $T > 135$ s) during inversion, thus combining waveforms from different frequency bands (Duputel, Rivera, Kanamori, *et al.*, 2012; Ekström *et al.*, 2012). For larger earthquakes, Global CMT uses only mantle waves. Since 2010, the USGS uses the W phase for most inversions (Kanamori, 1993; Kanamori and Rivera, 2008; Hayes *et al.*, 2009). Of the 5000 earthquakes in our study, the USGS moment tensors were derived from the W phase for 4436 earthquakes (waves with periods of 50–2000 s),

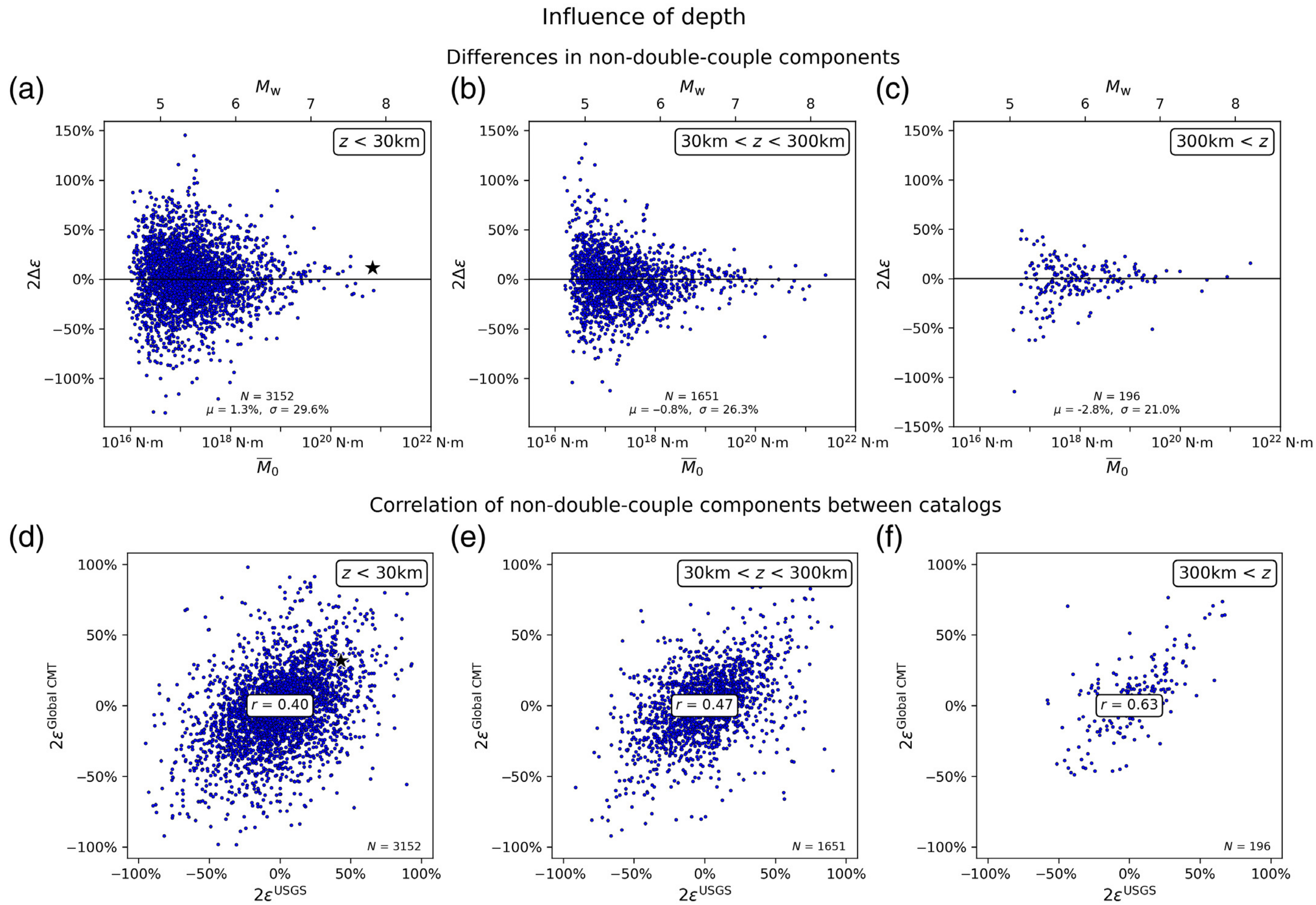

43 were determined from long-period surface waves (100–2000 s), 122 from long-period body waves (20–200 s), and those of 379 earthquakes were derived from an inversion of the surface-wave seismograms at regional distances (10–100 s). The moment tensors of 20 earthquakes were taken from catalogs other than the Global CMT catalog.

The inversions yield similar scalar moments, with Global CMT moments being generally larger. Because the *W* phase has significantly longer periods than used in many surface-wave studies (Kanamori, 1993), the differences in scalar moment may reflect the use of different phases during the inversion. Hayes *et al.* (2009) found that moment tensor inversions based on the *W* phase reproduce the magnitude obtained by Global CMT to within ±0.2 units for earthquakes with $M_w > 5.8$, equivalent to a difference in scalar moment of a factor of 2. This is consistent with the results for the 5000 earthquakes in our study (Fig. 13b). We also find an effect not noted by Hayes *et al.* (2009), namely generally higher magnitudes in the Global CMT catalog, especially for smaller earthquakes (Fig. 13a).

The small rotation angle between the DC components of source mechanisms in different catalogs suggests that fault angles are well determined. The correlation between NDC components in the two catalogs suggests that NDC components of small earthquakes are less certain and often spurious. However, when NDC components are consistent, they likely represent real source processes, either a deviation from a DC or source complexity producing an apparent NDC component.

The source mechanisms for large earthquakes agree better between catalogs than for small earthquakes, as shown by the decrease in scalar moment differences and rotation angles. This increased repeatability and thus presumable accuracy may result from several factors. For larger earthquakes, both the quantity and the quality of data available allow use of seismic waves recorded at many seismic stations worldwide with a high signal-to-noise ratio. Moreover, Earth models tend to agree better for the mantle than for the crust, for which 1D models show large deviations from 3D models. For larger earthquakes, we expect a decreased difference in moment tensors found using different Earth models for both elastic and anelastic structures. Thus, the source mechanisms reported

Figure 12. (a–c) Differences in NDC components and (d–f) correlation of NDC components for shallow ($z < 30$ km), intermediate (30 km $< z <$ 300 km), and deep earthquakes (300 km $< z$). The standard deviation of the differences in NDC components decreases, whereas the correlation between NDC components increases with centroid depth. The color version of this figure is available only in the electronic edition.

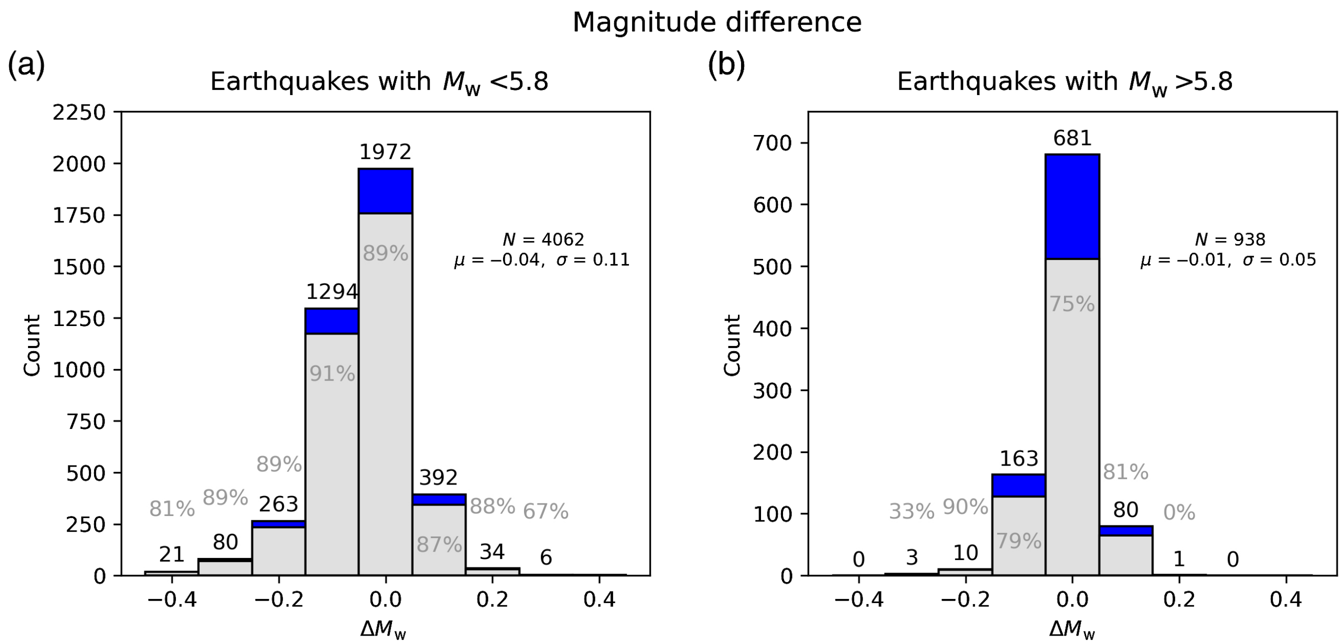

Figure 13. Magnitude differences (USGS–Global CMT) for earthquakes with (a) $M_w < 5.8$ and with (b) $M_w > 5.8$. The number of events and fraction of moment tensors determined using the *W* phase in each bin are shown. The color version of this figure is available only in the electronic edition.

in different catalogs should agree better for large earthquakes, despite different inversion procedures.

Data and Resources

The catalogs of centroid moment tensors used in this study are publicly accessible. The catalog of the Global Centroid Moment Tensor (Global CMT) Project (available at https://www.globalcmt.org, last accessed February 2021) formed the base of the dataset used in this study. For each event in the Global CMT catalog, we identified corresponding events with similar source time (±60 s), location (difference of less than 1°), and magnitude ($M_w \pm 0.5$) in the U.S. Geological Survey (USGS) catalog using the Python package ObsPy and its International Federation of Digital Seismograph Networks (FDSN) webservice client. The earthquakes in our dataset reach from the start of our search on 31 December 2020 until 3 November 2015. A list of the earthquakes including their source date and time and the corresponding moment tensors in both catalogs can be obtained upon request from the authors.

Declaration of Competing Interests

The authors acknowledge that there are no conflicts of interest recorded.

Acknowledgments

The authors thank Gavin Hayes, Paul Earle, Susan Hough, James Neely, Emile Okal, Norman Abrahamson, and Craig Bina for helpful discussions and two anonymous reviewers for thoughtful comments. This research was partially supported by U.S. Geological Survey Contract Number G19AC00104.

References

Cesca, S., E. Buforn, and T. Dahm (2006). Amplitude spectra moment tensor inversion of shallow earthquakes in Spain, *Geophys. J. Int.* **166,** no. 2, 839–854.

Cirella, A., A. Piatanesi, E. Tinti, M. Chini, and M. Cocco (2012). Complexity of the rupture process during the 2009 L'Aquila, Italy, earthquake, *Geophys. J. Int.* **190,** no. 1, 607–621.

d'Agostino, R. B. (1971). An omnibus test of normality for moderate and large size samples, *Biometrika* **58,** no. 2, 341–348.

Domingues, A., S. Custodio, and S. Cesca (2013). Waveform inversion of small-to-moderate earthquakes located offshore southwest Iberia, *Geophys. J. Int.* **192,** no. 1, 248–259.

Duputel, Z., L. Rivera, Y. Fukahata, H. Kanamori, and G. Hayes (2012). Uncertainty estimations for seismic source inversions, *Geophys. J. Int.* **190,** no. 2, 1243–1256.

Duputel, Z., L. Rivera, H. Kanamori, and G. Hayes (2012). *W* phase source inversion for moderate to large earthquakes (1990–2010), *Geophys. J. Int.* **189,** no. 2, 1125–1147.

Dziewonski, A. M., and J. Woodhouse (1983). An experiment in systematic study of global seismicity: Centroid-moment tensor solutions for 201 moderate and large earthquakes of 1981, *J. Geophys. Res.* **88,** no. B4, 3247–3271.

Dziewonski, A. M., T. A. Chou, and J. H. Woodhouse (1981). Determination of earthquake source parameters from waveform data for studies of global and regional seismicity, *J. Geophys. Res.* **86,** no. B4, 2825–2852.

Ekström, G., M. Nettles, and A. Dziewonski (2012). The Global CMT Project 2004–2010: Centroid-moment tensors for 13,017 earthquakes, *Phys. Earth Planet. In.* **200/201,** 1–9.

Engdahl, E. R., R. van der Hilst, and R. Buland (1998). Global teleseismic earthquake relocation with improved travel times and procedures for depth determination, *Bull. Seismol. Soc. Am.* **88,** no. 3, 722–743.

Ford, S. R., D. S. Dreger, and W. R. Walter (2010). Network sensitivity solutions for regional moment-tensor inversions, *Bull. Seismol. Soc. Am.* **100,** no. 5A, 1962–1970.

Frohlich, C., and S. D. Davis (1999). How well constrained are well-constrained T, B, and P axes in moment tensor catalogs?, *J. Geophys. Res.* **104,** no. B3, 4901–4910.

Giardini, D. (1984). Systematic analysis of deep seismicity: 200 centroid-moment tensor solutions for earthquakes between 1977 and 1980, *Geophys. J. Int.* **77,** no. 3, 883–914.

Gilbert, F. (1971). Excitation of the normal modes of the earth by earthquake sources, *Geophys. J. Int.* **22,** no. 2, 223–226.

Gilbert, F., and A. M. Dziewonski (1975). An application of normal mode theory to the retrieval of structural parameters and source mechanisms from seismic spectra, *Phil. Trans. Roy. Soc. London* **278,** no. 1280, 187–269.

Hamling, I. J., S. Hreinsdóttir, K. Clark, J. Elliott, C. Liang, E. Fielding, N. Litchfield, P. Villamor, L. Wallace, T. J. Wright, *et al.* (2017). Complex multifault rupture during the 2016 M_w 7.8 Kaikōura earthquake, New Zealand, *Science* **356,** no. 6334, doi: 10.1126/science.aam7194.

Harte, D., and D. Vere-Jones (1999). Differences in coverage between the PDE and New Zealand local earthquake catalogues, *New Zeal. J. Geol. Geophys.* **42,** no. 2, 237–253.

Hayes, G. P., R. W. Briggs, A. Sladen, E. J. Fielding, C. Prentice, K. Hudnut, P. Mann, F. W. Taylor, A. J. Crone, R. Gold, *et al.* (2010). Complex rupture during the 12 January 2010 Haiti earthquake, *Nature Geosci.* **3,** no. 11, 800–805.

Hayes, G. P., L. Rivera, and H. Kanamori (2009). Source inversion of the *W*-phase: Real-time implementation and extension to low magnitudes, *Seismol. Res. Lett.* **80,** no. 5, 817–822.

Hejrani, B., and H. Tkalčić (2020). Resolvability of the centroid-moment-tensors for shallow seismic sources and improvements from modeling high-frequency waveforms, *J. Geophys. Res.* **125,** no. 7, doi: 10.1029/2020JB019643.

Helffrich, G. R. (1997). How good are routinely determined focal mechanisms? Empirical statistics based on a comparison of Harvard, USGS and ERI moment tensors, *Geophys. J. Int.* **131,** no. 3, 741–750.

Jechumtálová, Z., and J. Šílený (2001). Point-source parameters from noisy waveforms: Error estimate by Monte-Carlo simulation, *Pure Appl. Geophys.* **158,** no. 9, 1639–1654.

Julian, B. R., and S. A. Sipkin (1985). Earthquake processes in the Long Valley caldera area, California, *J. Geophys. Res.* **90,** no. B13, 11, 155–11,169.

Julian, B. R., A. D. Miller, and G. R. Foulger (1998). Non-double-couple earthquakes 1. Theory, *Rev. Geophys.* **36,** no. 4, 525–549.

Kagan, Y. Y. (1991). 3-D rotation of double-couple earthquake sources, *Geophys. J. Int.* **106,** no. 3, 709–716.

Kagan, Y. Y. (2003). Accuracy of modern global earthquake catalogs, *Phys. Earth Planet. In.* **135,** nos. 2/3, 173–209.

Kanamori, H. (1993). *W* phase, *Geophys. Res. Lett.* **20,** no. 16, 1691–1694.

Kanamori, H., and J. W. Given (1981). Use of long-period surface waves for rapid determination of earthquake-source parameters, *Phys. Earth Planet. In.* **27,** no. 1, 8–31.

Kanamori, H., and L. Rivera (2008). Source inversion of *W*-phase: Speeding up seismic tsunami warning, *Geophys. J. Int.* **175,** no. 1, 222–238.

Kawakatsu, H. (1991). Enigma of earthquakes at ridge-transform-fault plate boundaries distribution of non-double couple parameter of Harvard CMT solutions, *Geophys. Res. Lett.* **18,** no. 6, 1103–1106.

Knopoff, L., and M. J. Randall (1970). The compensated linear-vector dipole: A possible mechanism for deep earthquakes, *J. Geophys. Res.* **75,** no. 26, 4957–4963.

McCowan, D. W. (1976). Moment tensor representation of surface wave sources, *Geophys. J. Int.* **44,** no. 3, 595–599.

Mendiguren, J. A. (1977). Inversion of surface wave data in source mechanism studies, *J. Geophys. Res.* **82,** no. 5, 889–894.

Miller, A. D., G. R. Foulger, and B. R. Julian (1998). Non-double-couple earthquakes 2. Observations, *Rev. Geophys.* **36,** no. 4, 551–568.

Neely, J. S., S. Stein, and B. D. Spencer (2020). Large uncertainties in earthquake stress-drop estimates and their tectonic consequences, *Seismol. Res. Lett.* **91,** no. 4, 2320–2329.

Nettles, M., and G. Ekström (1998). Faulting mechanism of anomalous earthquakes near Bárdarbunga Volcano, Iceland, *J. Geophys. Res.* **103,** no. B8, 17,973–17,983.

Röhm, A. H. E., J. Trampert, H. Paulssen, and R. K. Snieder (1999). Bias in reported seismic arrival times deduced from the ISC bulletin, *Geophys. J. Int.* **137,** no. 1, 163–174.

Rößler, D., F. Krüger, and G. Rümpker (2007). Retrieval of moment tensors due to dislocation point sources in anisotropic media using standard techniques, *Geophys. J. Int.* **169,** no. 1, 136–148.

Silver, P. G., and T. H. Jordan (1982). Optimal estimation of scalar seismic moment, *Geophys. J. Int.* **70,** no. 3, 755–787.

Sipkin, S. A. (1986). Interpretation of non-double-couple earthquake mechanisms derived from moment tensor inversion, *J. Geophys. Res.* **91,** no. B1, 531–547.

Smith, G. P., and G. Ekström (1997). Interpretation of earthquake epicenter and CMT centroid locations, in terms of rupture length and direction, *Phys. Earth Planet. In.* **102,** nos. 1/2, 123–132.

Storchak, D. A., A. L. Bird, and R. D. Adams (2000). Discrepancies in earthquake location between ISC and other agencies, *J. Seismol.* **4,** no. 3, 321–331.

Šílený, J. (2004). Regional moment tensor uncertainty due to mismodeling of the crust, *Tectonophysics* **383,** nos. 3/4, 133–147.

Šílený, J., P. Campus, and G. F. Panza (1996). Seismic moment tensor resolution by waveform inversion of a few local noisy records—I. Synthetic tests, *Geophys. J. Int.* **126,** no. 3, 605–619.

Vavryčuk, V. (2015). Moment tensor decompositions revisited, *J. Seismol.* **19,** no. 1, 231–252.

Vera Rodriguez, I., Y. J. Gu, and M. D. Sacchi (2011). Resolution of seismic-moment tensor inversions from a single array of receivers, *Bull. Seismol. Soc. Am.* **101,** no. 6, 2634–2642.

Wallace, T. (1985). A reexamination of the moment tensor solutions of the 1980 Mammoth Lakes earthquakes, *J. Geophys. Res.* **90,** no. B13, 11,171–11,176.

Manuscript received 11 March 2021
Published online 2 June 2021